

# Quantum Electronics Letters

## Interband Auger Recombination in InGaAsP

L. C. CHIU, P. C. CHEN, AND AMNON YARIV

**Abstract**—The interband Auger recombination lifetimes of two Auger processes have been calculated to correlate measured threshold current densities and carrier lifetimes for InGaAsP and InGaAsSb lasers. Good agreement with experimental data was obtained for lasers with low nominal threshold current densities. These results demonstrate the importance of Auger recombination in the threshold characteristics of InGaAsP/InP lasers.

SEMICONDUCTOR injection lasers using the quaternary compound InGaAsP as active layers generally exhibit threshold current densities that depend strongly on temperature. They are characterized by a low  $T_0$  ranging from 50–80 K for temperatures above about 220 K [1]–[3]. This value is considerably lower than that of GaAlAs/GaAs lasers, which is typically greater than 110 K. Low values of  $T_0$  pose serious limitations on the performance of semiconductor lasers at elevated temperatures. It is therefore important to understand the origin and nature of this phenomenon in the quaternary InGaAsP/InP lasers.

For the InGaAsP lasers, the onset of the rapid increase in threshold current with ascending temperature at about 220–250 K is accompanied by a sharp decrease in the carrier lifetime and the spontaneous recombination efficiency [1], [3], [7], [8]. Various mechanisms have been proposed to account for the reduction in carrier lifetime [1], [4], [6] of which the nonradiative Auger recombination has received special attention [7]–[10]. Fig. 1 shows two Auger recombination processes that should be significant at high temperatures for small bandgap semiconductors [11], [13]. In this letter we present calculations of the nonradiative Auger lifetime due to these two Auger processes, referred to as CHCC and CHSH processes, which involve electrons/holes in the conduction/valence bands and conduction/split-off hole bands. The CHCC process was discussed in [8]. However, the expression used in [8] was derived under the assumptions that both the conduction and the valence bands are nondegenerate, and that the injection level is low. Since semiconductor lasers operate under high injection condition which renders the conduction band degenerate, neither of the above assumptions is made in the present

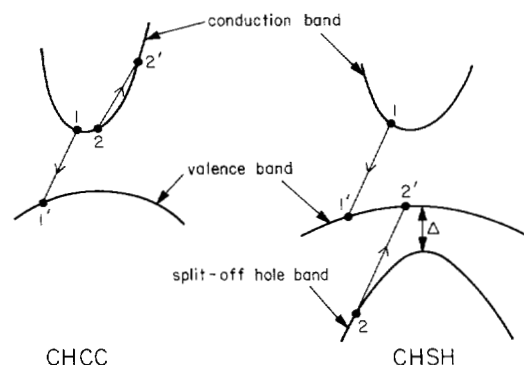


Fig. 1. The CHCC and CHSH Auger recombination processes. 1, 2 and 1', 2' are the initial and final states, respectively.

calculation. The CHSH process has been treated in [10], and the formalism used here is similar. However, owing to the inadequate accuracy with which the parameters needed for gain calculations are known, we elected not to calculate theoretically the injected carrier density at threshold  $n_{th}$  from the balance between gain and loss, but instead, to obtain  $n_{th}$  from existing experimental measurements of the threshold current density  $J_{th}$ , and carrier lifetime  $\tau$  as functions of temperature by applying the relation

$$\frac{J_{th}}{ed} = \frac{n_{th}}{\tau}$$

where  $e$  is the electronic charge and  $d$  is the active layer thickness. This procedure would yield accurate values of  $n_{th}$  for high quality lasers with low nominal threshold current density  $J_{th}/d$ .

The rate  $P$  for the band-to-band Auger recombination is given by [11]

$$P = \frac{2\pi}{\hbar} (2\beta)^2 \left( \frac{V}{(2\pi)^3} \right)^3 \left( \frac{e^2}{\epsilon V} \right)^2 \iiint \frac{|F_1 F_2|^2}{(|\mathbf{k}_1 - \mathbf{k}_1'|^2 + L_D^{-2})^2} \times [f_1 f_2 (1 - f_1')(1 - f_2') - (1 - f_1)(1 - f_2) f_1' f_2'] \cdot \delta(E_f - E_i) d\mathbf{k}_1 d\mathbf{k}_1' d\mathbf{k}_2'.$$

In the above, the  $f$ 's are the Fermi factors,  $E_{f,i}$  are the final and initial energies of the particles, respectively,  $L_D$  is the usual screening length, and  $2 < 2\beta < 3$  [11] due to spin sym-

Manuscript received June 24, 1981. This work was supported by the National Science Foundation and the Office of Naval Research.

The authors are with the California Institute of Technology, Pasadena, CA 91125.

TABLE I  
COMPARISON OF MEASURED AND CALCULATED CARRIER LIFETIMES FOR  
InGaAsP LASERS AT 300 K. BETTER AGREEMENT IS OBTAINED FOR  
LASERS WITH LOW  $J_{th}/d$ .

| Wavelength ( $\mu\text{m}$ ) | $J_{th}/d$ ( $\text{kA}/\text{cm}^2\mu\text{m}$ ) | $\tau_{exp}$ (ns) | $\tau_{cal}$ (ns) |
|------------------------------|---|-------------------|-------------------|
| 1.1                          | -   | 4.0               | 4.2               |
| 1.27                         | 14.0  | 2.0               | 1.4               |
| 1.3                          | 9.0   | 2.3               | 2.0               |
| 1.48                         | 7.8   | 1.7               | 2.0               |

metry. The overlap integrals  $|F_1 F_2|^2$  are given by

$$|F_1 F_2|^2 \doteq \frac{\hbar^2}{2m_e E_g} f_{CV} |\mathbf{k}_1 - \mathbf{k}_1'|^2$$

for the CHCC process [12] and

$$|F_1 F_2|^2 \doteq \alpha_{CH} \alpha_{SH} \frac{|\mathbf{k}_1 - \mathbf{k}_1'|^2}{E_g^2}$$

for the CHSH [10], [13] process. In the above equations,  $m_e$  is the electron mass,  $E_g$  is the bandgap energy, and  $f_{CV}$  is the oscillator strength. The  $\alpha_{CH}$  and  $\alpha_{SH}$  are the overlap parameters as given in [10]. The effective masses for electron and hole, and the spin-orbit coupling  $\Delta$  are taken from [15] and [16], respectively. The three-fold integrations were calculated numerically assuming parabolic bands, and the Auger lifetime is obtained from the expression

$$\tau_A = \frac{\Delta n}{P}$$

where  $\Delta n$  is the injected carrier density at threshold. In the calculation, the Fermi levels are calculated from experimental values of  $n_{th}$ , when degeneracy is fully accounted for in the conduction band. It is also assumed that injection level is high, so that  $\Delta n \doteq n_{th}$ , an assumption which is good for injection lasers.

Data for lasers emitting at 1.1, 1.27, 1.3, and 1.48  $\mu\text{m}$  were taken, respectively, from [1], [3], [8], and [7]. To account for current spreading under the stripes, the measured  $J_{th}$  was divided by factors of 1.6 and 1.2 as appropriate for 15 and 20  $\mu\text{m}$  stripes to obtain the actual current density in the active region [17].

For comparison, the calculated and experimental carrier lifetime at 300 K are listed in Table I, along with other characteristics of the lasers. The total carrier lifetime is obtained from the sum of the radiative and Auger effects by

$$\frac{1}{\tau} = \frac{1}{\tau_{rad}} + \frac{1}{\tau_{CHCC}} + \frac{1}{\tau_{CHSH}}$$

The radiative lifetime is obtained by extrapolation of experimental values at low temperatures. As is evident from Table I and Figs. 2-5, reasonable agreement was obtained for lasers with low nominal threshold current density. When the nominal threshold current density is high, the calculated Auger lifetimes are significantly shorter than the observed values. This is due to the high apparent carrier concentration resulting from the

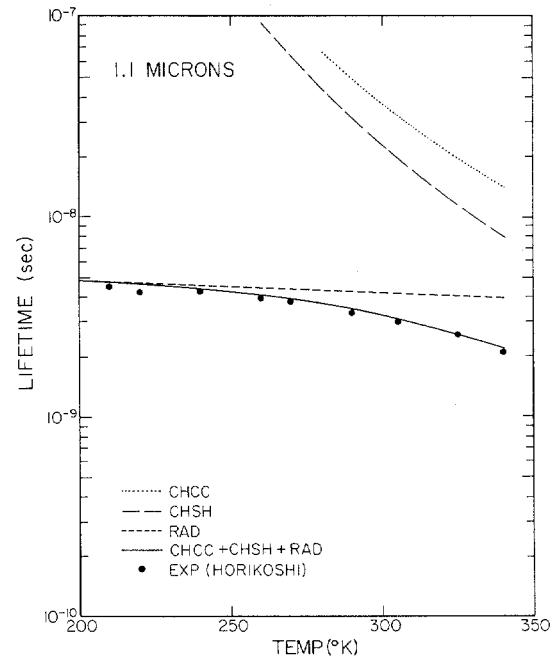


Fig. 2. Calculated and measured lifetimes of 1.1  $\mu\text{m}$  laser. Data taken from [1].

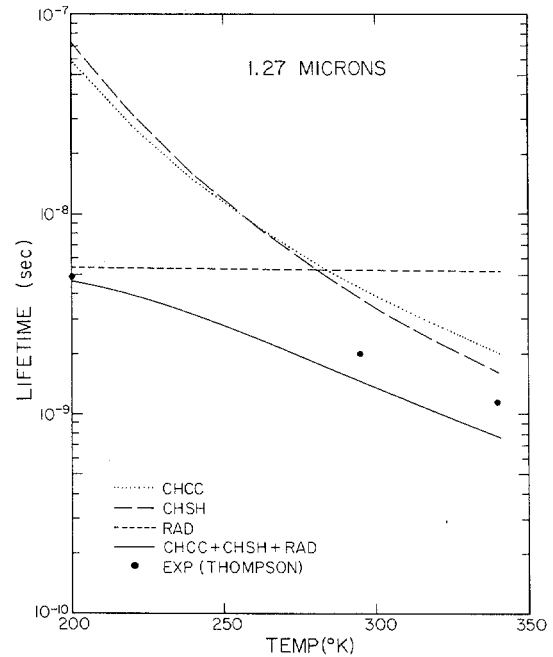


Fig. 3. Calculated and measured lifetimes of 1.27  $\mu\text{m}$  laser. Data taken from [3].

high threshold current density, which implies the existence of additional current loss mechanisms not accounted for here. It should be cautioned that the Auger lifetime is a rather sensitive function of carrier concentration (see Fig. 6), and calculations are meaningful only if reliable values of  $n_{th}$  can be obtained.

We have also examined the phonon-assisted Auger recombinations. It has been proposed that these processes are important in semiconductors at low temperatures, since the participation of a phonon relaxes the requirement of simultaneous energy and momentum conservation of the electrons and holes

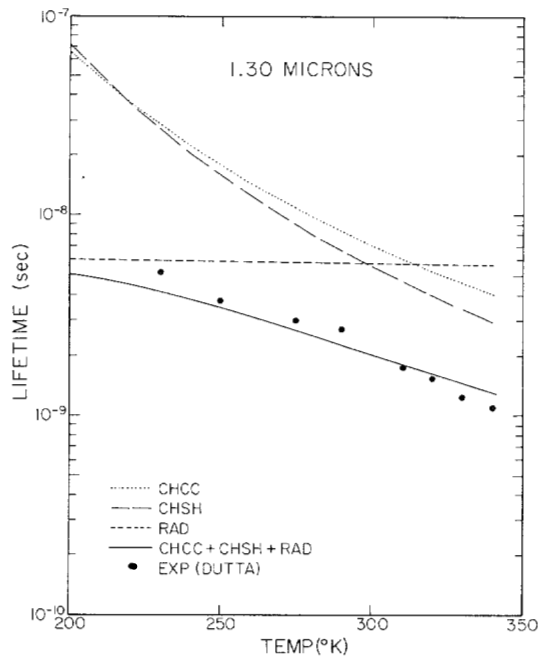


Fig. 4. Calculated and measured lifetimes of 1.3  $\mu\text{m}$  laser. Data taken from [8].

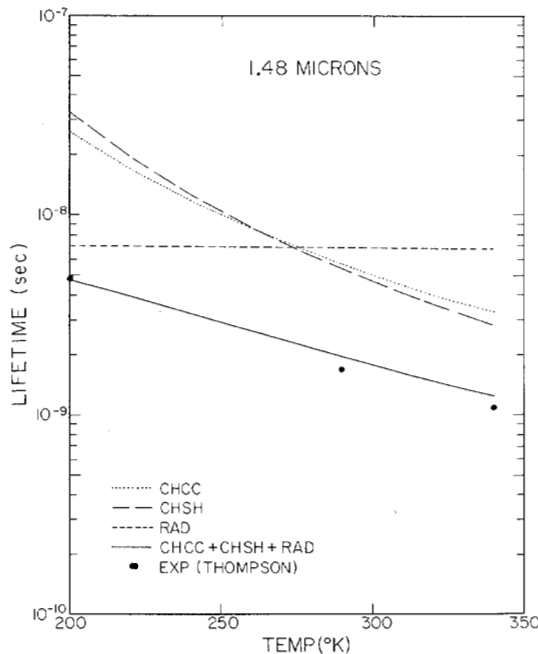


Fig. 5. Calculated and measured lifetimes of 1.48  $\mu\text{m}$  laser. Data taken from [7].

[18]. Our preliminary calculations show that while the Auger lifetime of phonon-assisted CHCC and CHSH processes are shorter than the normal CHCC and CHSH processes at low temperatures (<150 K), they are at least an order of magnitude longer above 200 K. Therefore, their contribution to the total carrier lifetime can be neglected.

The Auger lifetime is known to vary approximately with the carrier concentration as

$$\frac{1}{\tau} \sim n^a$$

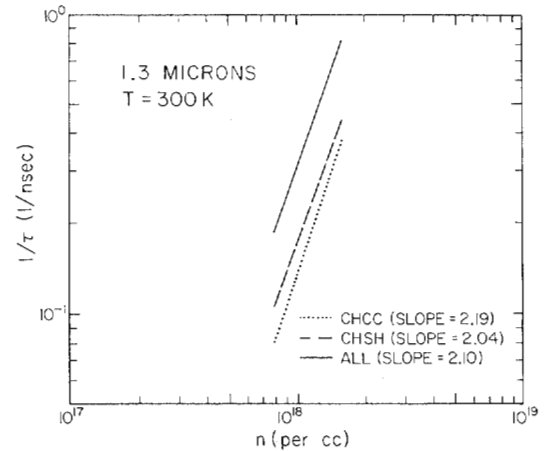


Fig. 6. The inverse of Auger lifetime as a function of carrier concentration for a 1.3  $\mu\text{m}$  InGaAsP laser at 300 K.

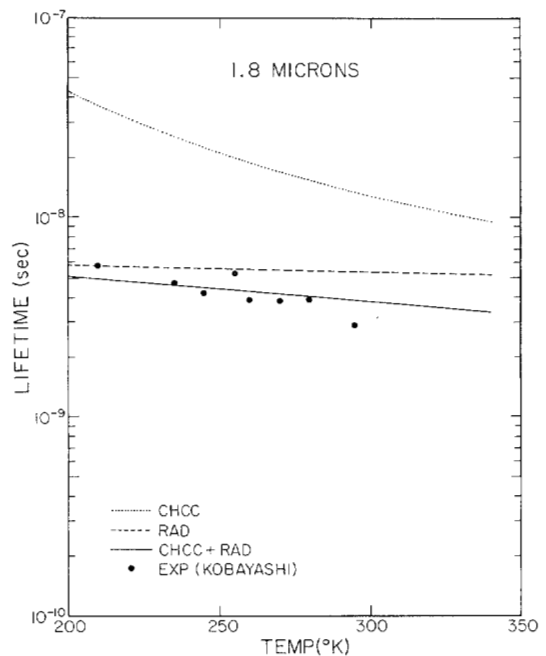


Fig. 7. Calculated and measured lifetimes of 1.8  $\mu\text{m}$  InGaAsSb laser. Data taken from [20].

where  $a$  is between 2 and 4. By varying  $n$ , we have plotted  $1/\tau$  versus  $n$  for a 1.3  $\mu\text{m}$  laser at 300 K (Fig. 6) on a log-log scale. The slopes of the lines indicate that  $a = 2.19$  for the CHCC process and  $a = 2.04$  for the CHSH process. The combined nonradiative Auger lifetime varies with  $n^{2.10}$ . This compares favorably with the value of 2.2 obtained on LED experiments by Uji *et al.* [19].

The Auger lifetime for an InGaAsSb/GaAlAsSb laser emitting at 1.8  $\mu\text{m}$  has also been calculated. The data for this laser are taken from [20]. Since limited information is available, linear interpolation is taken between the binary compounds of GaAs, InAs, and InSb to obtain the relevant parameters needed. One interesting result worth mentioning is that the lifetime for the CHSH process is about two orders of magnitude longer than the CHCC process. This we believe is due to the large  $\Delta$  in this system. The calculated and experimental values are compared in Fig. 7, and reasonable agreement exists. However, since

the band parameters used here are less accurate as those in the InGaAsP/InP system, the result presented here should only be regarded as preliminary. An interesting property of this laser is its high  $T_o$  ( $\sim 112$  K), which may be due partially to the absence of the CHSH process. It should be pointed out that nonradiative Auger recombination cannot explain the decrease in differential quantum efficiency in this laser [20].

### CONCLUSIONS

In conclusion, it has been demonstrated that the Auger lifetime for both CHCC and CHSH process are comparable in the temperature range of 200–340 K. Reasonable agreement was obtained for the measured and calculated lifetimes of low threshold lasers emitting from 1.1 to 1.48  $\mu\text{m}$ . Results indicate that the nonradiative Auger recombination is an important factor responsible for the high temperature sensitivity of the threshold current of InGaAsP/InP quaternary lasers.

### REFERENCES

- [1] Y. Horikoshi and Y. Furukawa, "Temperature sensitive threshold current of InGaAsP-InP double heterostructure lasers," *Japan. J. Appl. Phys.*, vol. 18, no. 4, pp. 809–815, 1979.
- [2] Y. Horikoshi, H. Saito, M. Kawashima, and T. Takanashi, "Low-temperature behavior of the threshold current and carrier lifetime of InGaAsP-InP DH lasers," *Japan. J. Appl. Phys.*, vol. 18, no. 8, pp. 1657–1658, 1979.
- [3] G.H.B. Thompson and G. Henshall, "Nonradiative carrier loss and temperature sensitivity of threshold in 1.27  $\mu\text{m}$  (GaIn)(AsP)/InP D.H. lasers," *Electron. Lett.*, vol. 16–11, no. 1, pp. 42–44, 1980.
- [4] M. Ettenberg, M. Nuege, and H. Kressel, "The temperature dependence of threshold current for double-heterojunction lasers," *J. Appl. Phys.*, vol. 50, pp. 2949–2950, 1979.
- [5] A. Adams, M. Asada, Y. Suematsu, and S. Arai, "The temperature dependence of the efficiency and threshold current of InGaAsP lasers related to intervalence band absorption," *Japan. J. Appl. Phys.*, vol. 19, no. 10, pp. L621–624, 1980.
- [6] M. Asada, A. Adams, K. Stubkjaer, Y. Suematsu, Y. Itaya, and S. Arai, "The temperature dependence of the threshold current of GaInAsP/InP DH lasers," *IEEE J. Quantum Electron.*, vol. QE-17, pp. 611–618, May 1981.
- [7] G.H.B. Thompson, "Temperature dependence of threshold current in (GaIn)(AsP)/InP DH lasers at 1.3 and 1.5  $\mu\text{m}$  wavelength," *Proc. Inst. Elec. Eng.*, vol. 128, no. 2, pp. 37–43, 1981.
- [8] N. Dutta and R. Nelson, "Temperature dependence of threshold of InGaAsP/InP double-heterostructure lasers and Auger recombination," *Appl. Phys. Lett.*, vol. 38, no. 6, pp. 407–409, 1981.
- [9] A. Sugimura, "Band-to-band Auger effect on the output power saturation in InGaAsP LED's," *IEEE J. Quantum Electron.*, vol. QE-17, pp. 441–444, Apr. 1981.
- [10] —, "Band-to-band Auger recombination effect on InGaAsP laser threshold," *IEEE J. Quantum Electron.*, vol. QE-17, pp. 627–635, May 1981.
- [11] A. R. Beattie and P. T. Landsberg, "Auger effect in semiconductors," *Proc. Roy. Soc. Ser. A*, vol. 249, pp. 16–29, 1958; also in L. Hultdt, "Auger recombination in germanium," *Phys. Status. Solidi. (a)*, vol. 24, pp. 221–229, 1974.
- [12] E. Antoncik and P. T. Landsberg, "Overlap integrals for Bloch electrons," *Proc. Phys. Soc. London*, vol. 82, pp. 337–342, 1963.
- [13] M. Takeshima, "Auger recombination in InAs, GaSb, InP, and GaAs," *J. Appl. Phys.*, vol. 43, no. 10, pp. 4114–4119, 1972.
- [14] A. Sugimura, "Band-to-band Auger effect in GaSb and InAs lasers," *J. Appl. Phys.*, vol. 51, no. 8, pp. 4405–4441, 1980.
- [15] N. K. Dutta, "Gain-current relation for  $\text{In}_{0.72}\text{Ga}_{0.28}\text{As}_{0.6}\text{P}_{0.4}$  lasers," *J. Appl. Phys.*, vol. 52, no. 1, pp. 55–60, 1981.
- [16] Y. Yamazoe, T. Nishino, and Y. Hamakawa, "Electroreflectance study of GaInAsP quaternary alloys lattice matched to InP," *IEEE J. Quantum Electron.*, vol. QE-17, pp. 139–144, Feb. 1981.
- [17] J. J. Hsieh and C. C. Shen, "Room temperature CW operation of buried-stripe double-heterostructure GaInAsP/InP diode lasers," *Appl. Phys. Lett.*, vol. 30, pp. 429–431, 1977.
- [18] A. Haug, "Phonon-assisted Auger recombination in degenerate semiconductors," *Solid State Commun.*, vol. 22, pp. 537–539, 1977, and references therein.
- [19] T. Uji, K. Iwanoto, and R. Lang, "Nonradiative recombination in InGaAsP/InP light sources causing light emitting diode saturation and strong laser-threshold-current temperature sensitivity," *Appl. Phys. Lett.*, vol. 38, no. 4, pp. 193–195, 1981.
- [20] N. Kobayashi, Y. Horikoshi, and C. Uemura, "Room temperature operation of the InGaAsSb/AlGaAsSb DH laser at 1.8  $\mu\text{m}$  wavelength," *Japan. J. Appl. Phys.*, vol. 19, no. 1, pp. L30–32, 1980.

## Efficiency Studies of the Thallium Anti-Stokes Raman Laser

JONATHAN C. WHITE AND D. HENDERSON

**Abstract**—Selective photodissociation of TlCl and TlI using 248 nm radiation from a KrF\* excimer laser has been used to create a  $\text{Tl}^*(6p^2P_{3/2}^\circ)$  metastable state population inversion. Stimulated anti-Stokes Raman emission at 376 nm has been observed using a 532 nm pump laser. Output power at the anti-Stokes wavelength and conversion efficiencies are reported.

### INTRODUCTION

IN this letter we report studies of the Tl anti-Stokes Raman laser in which new methods for creating the necessary  $\text{Tl}^*(6p^2P_{3/2}^\circ)$  population inversion have been investigated. The first observation of stimulated anti-Stokes Raman emission was performed by preparing a  $\text{Tl}^*(6p^2P_{3/2}^\circ)$  metastable inversion with respect to the ground state of Tl by selective photodissociation of TlCl by a 193 nm photon from an ArF\* excimer

Manuscript received February 5, 1982.

The authors are with Bell Laboratories, Holmdel, NJ 07733.